Proc. Natl. Acad. Sci. USA
Vol. 92, pp. 8279–8282, August 1995
Neurobiology

Two types of calcium response limited to single spines in cerebellar Purkinje cells

(6-cyano-7-nitroquinoxaline-2,3-dione/Calcium Green/glutamate receptor/brain slices)

WINFRIED DENK*, MUTSUYUKI SUGIMORI†, AND RODOLFO LLINÁS†

*Biological Computation Research Department, AT&T Bell Laboratories, Murray Hill, NJ 07974; and †Department of Physiology and Neuroscience, New York University Medical Center, New York, NY 10016

Contributed by Rodolfo Llinás, June 2, 1995

ABSTRACT **Of fundamental importance in understanding neuronal function is the unambiguous determination of the smallest unit of neuronal integration. It was recently suggested that a whole dendritic branchlet, including tens of spines, acts as the fundamental unit in terms of dendritic calcium dynamics in Purkinje cells. By contrast, we demonstrate that the smallest such unit is the single spine. The results show, by two-photon excited fluorescence laser scanning microscopy, that individual spines are capable of independent calcium activation. Moreover, two distinct spine populations were distinguished by their opposite response to membrane hyperpolarization. Indeed, in a subpopulation of spines calcium entry can also occur through a pathway other than voltage-gated channels. These findings challenge the assumption of a unique parallel fiber activation mode and prompt a reevaluation of the level of functional complexity ascribed to single neurons.**

It is now well established that the dendrites of Purkinje cells are capable of a voltage-dependent regenerative calcium response (1–6). Recently, it was further demonstrated that, after parallel fiber activation, a spiny branchlet with its associated spines can fire as a unit (7). By this account, the branchlet would be the site of spike generation, followed by the retrograde invasion of spines from the parent branchlet.

Here we present direct evidence that Purkinje cell spines, as those in pyramidal cells (8), can respond as single electrical and calcium concentration compartments to parallel fiber synaptic activation. The results indicate, therefore, that the smallest unit of active electrical response is the spine, rather than the spiny branchlet, and thus the spine has to be considered the fundamental unit in Purkinje cell integration (9). We also show two distinct types of spine synaptic responses during somatic hyperpolarization. These results are consistent with the recent finding of two types of spines showing segregation of receptors (10) in mice lacking the δ2 subunit of the Purkinje cell glutamate receptor (GluRδ2).

MATERIALS AND METHODS

Purkinje cells were imaged by two-photon excited fluorescence laser scanning microscopy (11, 12), which allows the measurement of calcium concentration changes at the level of single spines (8). Neurons were whole-cell voltage clamped at the soma (Fig. 1). Calcium Green (Molecular Probes) was allowed to diffuse from the patch pipette to fill the entirety of the cytosol so that the whole dendritic tree, down to the level of single spines, could be visualized (Fig. 2*a*). Functional imaging of single spines and spiny branchlets was then performed at higher magnification levels (Fig. 2 *b–d*), using a ×63/0.9 numerical aperture water immersion objective. Electrical stimulation of parallel fibers was implemented at the molecular layer in the vicinity of a spiny branchlet (Fig. 1). The stimulating probe, a saline-filled glass pipette with a 2-μm tip diameter was placed ≈10 μm above the plane of the Purkinje cell dendrite. Given the spatial organization of the parallel fibers, this location ensured that synaptic activation would occur within the comparatively small field of view over which fast, high-resolution imaging could be performed. Purkinje cells were usually held at −80 mV, but during given experiments the holding potential was modified to levels between −55 and −280 mV (nominally). Experiments were performed at room temperature (25°C) in 250-μm-thick guinea pig cerebellar slices by standard procedures. The extracellular solution contained 124 mM NaCl, 5 mM KCl, 1.2 mM KH_2PO_4, 1.3 mM $MgSO_4$, 26 mM $NaHCO_3$, 10 mM dextrose, and 2.4 mM $CaCl_2$, equilibrated with 5% CO_2/95% O_2. The recording pipette solution contained 130 mM potassium methanesulfonate, 10 mM Hepes, 2 mM $MgCl_2$, 5 mM Na_2ATP, and 0.125 mM Calcium Green-K_6. Heat-polished recording pipettes (borosilicate) had a preseal resistance of 5 MΩ. No series resistance compensation was used. Laser scanning was performed with a modified MRC600 laser scanning microscope with a custom-

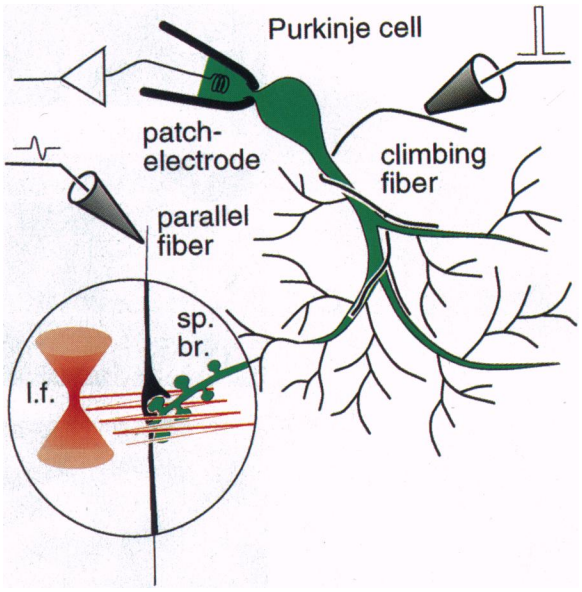

FIG. 1. Diagram of the experimental design. Purkinje cell whole-cell clamped at the soma and filled with Calcium Green by diffusion. Stimulating electrodes (saline filled micropipettes) activate parallel fibers or climbing fibers. Images are generated by raster scanning a focused laser beam (l.f.) across spiny branchlets (sp. br.), while fluorescence generated by two-photon excitation in the focus is detected and used as the contrast signal.

The publication costs of this article were defrayed in part by page charge payment. This article must therefore be hereby marked "*advertisement*" in accordance with 18 U.S.C. §1734 solely to indicate this fact.

Abbreviations: CNQX, 6-cyano-7-nitroquinoxaline-2,3-dione; GluRδ2, δ2 subunit of glutamate receptor.

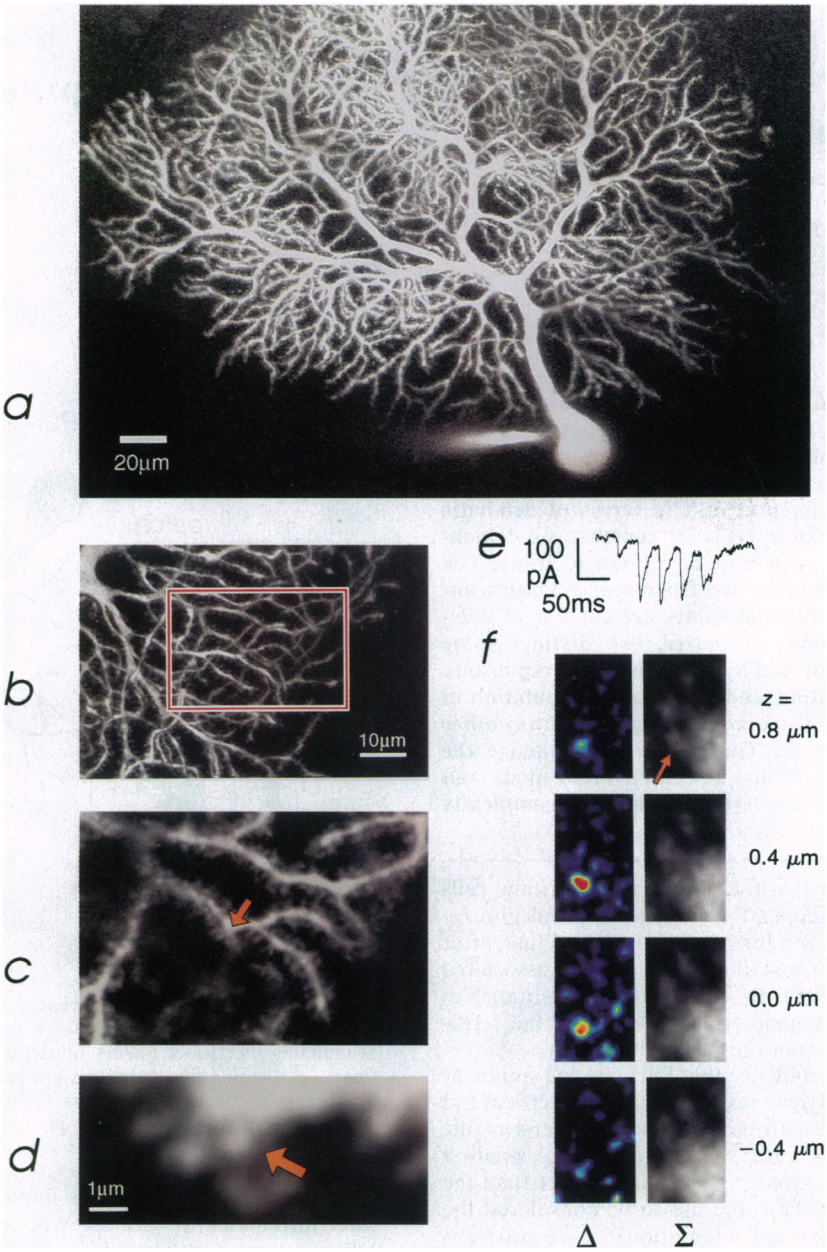

FIG. 2. Single spine activation via parallel fiber stimulation. After Calcium Green diffusion from the patch electrode, a complete Purkinje cell dendritic tree (*a*) is shown. Functional imaging was performed in a different cell, which is shown at three magnifications (*b*, *c*, and *d*). Note that single spines are well resolved. (*a–d*) Maximal value projections of a stack of optical sections. In *c* and *d*, the actual spine activated in *e* is indicated by arrows. A train of low-amplitude parallel fiber stimuli generated small subthreshold synaptic currents (*e*) at the soma. In *f*, difference images (stimulated − resting; Δ) and the resting fluorescence level (Σ) taken at four different depths show the single spine calcium response produced by the parallel fiber stimuli.

built compound microscope and whole-field detection (13) using a photomultiplier (Hamamatsu, Middlesex, NJ; model 9836) with a colored glass filter (BG39; Schott, Mainz, F.R.G.) for excitation rejection. The light source for two-photon excitation was a Ti/sapphire laser (λ = 840–860 nm; 100-fs pulses at 100 MHz; average power, <50 mW at the sample).

RESULTS

Single or multiple electrical stimuli to the parallel fiber (Fig. 2) produced well-resolved synaptic currents (Fig. 2*e*) under whole-cell patch-clamp conditions. To determine whether such local stimuli evoked a cytosolic calcium concentration increase in the Purkinje cell, changes in Calcium Green fluorescence were monitored. The level of spatial resolution achieved is illustrated for a particular cell (Fig. 2 *a–d*) at different magnifications to show the site of functional imaging in relation to the rest of the cell and to demonstrate the clarity with which single spines can be resolved. After parallel fiber activation, areas of changing calcium concentration were identified by subtracting an image of the resting fluorescence taken immediately beforehand from a Calcium Green fluorescence image taken during parallel-fiber stimulation. To ensure that an activated spine would be detected irrespective of its position in the scan area (Fig. 2*f*), a brief train of pulses was used (four or five pulses at 50 Hz), with scanning starting at the time of the second stimulus. Frequently, Purkinje cells (n = 18) responded with well-resolved fluorescence changes that were, at low stimulus intensities, restricted to a single spine or a small number of well-separated spines, with little activation in the

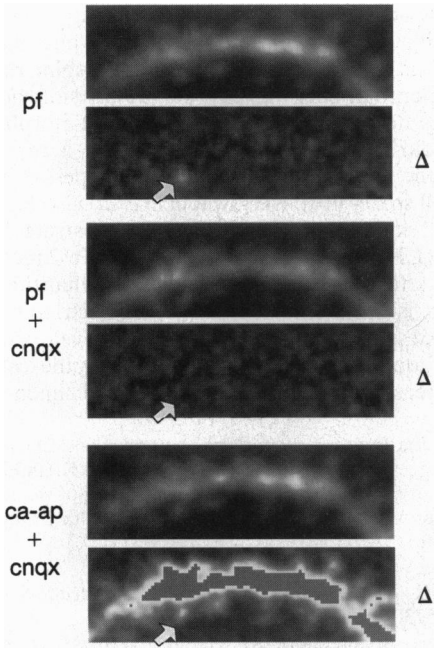

FIG. 3. Glutamatergic nature of single spine activation. Parallel fiber stimulation activates single spine (pf). After adding CNQX, the response is suppressed (pf+cnqx) but the branchlet still responds to calcium spikes triggered by somatic depolarization (ca-ap+cnqx). Arrows indicate positions of the spine.

intervening branchlet shaft (see Fig. 4*a*). That the response was confined to isolated spines was further confirmed by repeating the experiment at different focal plane settings. This is illustrated in Fig. 2*f*, where a single spine is seen to change in the difference images [Fig. 2*f Left* (Δ), in pseudocolor]. The spine location is indicated by arrows in Fig. 2 *c, d*, and *f*. As in Fig. 2*d*, changes could usually be identified over a focal range of 1–1.5 μm, indicating a small source with its apparent vertical extent determined mainly by the optical resolution along the *z* axis. Note that neither the supporting dendritic branchlet nor the neighboring spines show a difference signal above noise level.

To determine whether the activation of isolated spines was due to parallel fiber synaptic input, the glutamate channel blocker 6-cyano-7-nitroquinoxaline-2,3-dione (CNQX) was added to the bath after recording a clear single spine response (Fig. 3, pf) using the difference-image method described above. In the presence of CNQX, the same stimulus failed to produce a response (Fig. 3, pf + cnqx). However, somatic stimulation capable of generating a calcium-dependent spike (ca-ap + cnqx) produced a clear activation of the same and all neighboring spines as well as of the supporting branchlet, demonstrating that CNQX had not reduced voltage-activated calcium conductances in the neuron. Additional evidence for the synaptic origin is the finding that neighboring spines fail independently of each other (data not shown).

While the results in Figs. 2 and 3 demonstrate that single spines can be individually activated via parallel fiber stimulation, it was not clear whether calcium entered through voltage- or ligand-gated channels. Moreover, during the stimulus trains

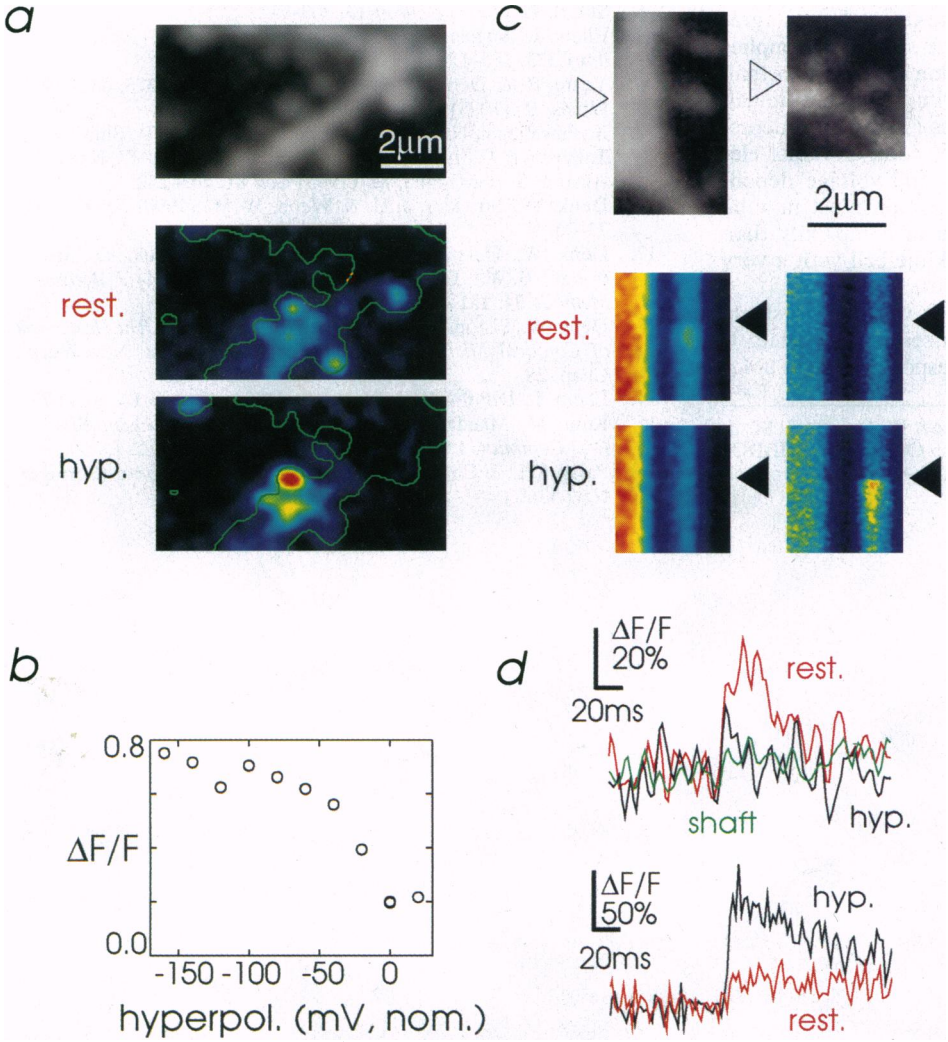

FIG. 4. Two populations of spines respond differently to hyperpolarization. (*a*) Response (pseudocolor difference images; stimulated − unstimulated) of a spiny branchlet (*Top*, gray scale image of morphology) is shown at normal holding potentials and when the cell was hyperpolarized (hyp.) during parallel fiber stimulation. Green outline serves as a reference for branchlet morphology. Note that two of the spines that were activated at the resting level failed to respond at hyperpolarized levels, while the response in the remaining spines increased. For a spine in a different cell, the increase in influx as a function of nominal hyperpolarization is shown in *b*, expressed as the fractional Calcium Green fluorescence increase ($\Delta F/F$) measured during a period of 20 ms after the stimulus. (*c*) Time-resolved line scans (in pseudocolor) are compared for spines with different behavior under hyperpolarization. (*Top*) Morphology is shown; open arrowheads indicate location of the line scanned. Solid arrowheads indicate stimulus time. (*Left*) Pictures (and top traces in *d*) show a spine with reduced influx. (*Right*) Spine (same as in *b*) with increased influx with hyperpolarization. Line plots in *d* show that calcium increases swiftly in all cases. For comparison, a time trace for the shaft is shown in green.

of up to 80 ms used for difference imaging, calcium could have been released from intracellular stores via a metabotropic inositol trisphosphate-mediated pathway (14). To address these issues, we first performed experiments at different holding potentials during synaptic stimulation. As shown in Fig. 4*a*, we found, to our surprise, that some spines ceased to respond when the cell was hyperpolarized, while in others the calcium response actually increased. Similar results were found when glutamate was applied iontophoretically, with calcium release from intracellular stores blocked by including heparin (500 μg/ml) (15) in the intracellular solution (data not shown).

To investigate further the possibility of calcium release from intracellular stores, rapid line scans (with 2-ms time resolution) were used to measure the calcium dynamics in spines during single parallel fiber stimuli (Fig. 4*c*). For both types of spines, the rate of increase of the calcium response was fast enough (2–3 ms; Fig. 4*d*) to exclude the slower chemical pathway (14) for the initial phase. This indicates that calcium must come from the extracellular space via voltage-sensitive calcium channels located in the spine heads‡ or through glutamate-dependent channels. The existence of spines that respond individually, but are sensitive to hyperpolarization, implies that a spine can be sufficiently isolated electrically to confine threshold membrane depolarization to itself without necessarily activating the adjacent shaft or neighboring spines. The issue of the transmission failures, which were sometimes observed with single shock parallel fiber stimulation, will be addressed in a separate publication.

DISCUSSION

Our experiments demonstrate that voltage-dependent integration already occurs at the level of a single spine. This implies that the granularity of dendritic integration is much finer than previously assumed—each of the 10^7 Purkinje cells in a human brain contains as many as 100,000 spines (30,000 in rodents) (16), providing the cerebellum with 10^{12} computational elements. Furthermore, given the kinetics and voltage dependence of calcium influx, dendritic integration must now be viewed as having a much larger degree of complexity than previously proposed, endowing the Purkinje cell with a very large number of possible functional states.

The functional significance of the two varieties of single spine calcium response is difficult to assess at this time. It seems possible that single spine electroresponsiveness is ubiquitous, with only a subset of spines showing calcium influx supported by glutamate-gated channels. While the voltage levels required to visualize the differences in spine response to somatic hyperpolarizing are beyond the physiological range, our findings do demonstrate a functional dimorphism. Furthermore, our findings are consistent with a recent report indicating the presence of at least two types of GluRs in Purkinje cell spines (10). Kashiwabuchi *et al.* also indicate that the GluRδ2 knockout mice fail to demonstrate long-term depression (LTD) and conclude that the GluRδ2 receptors are the substrate for LTD. While it is not clear that this receptor dimorphism is related to the functional dichotomy that we report here, especially since we used fully developed animals, this issue should be resolved when single spine calcium dynamics is measured in GluRδ2 knockout specimens.

‡Hillman, D., Chen, S., Aung, T. T., Cherksey, B., Sugimori, M. & Llinás, R. Third International Brain Research Organization (IBRO) World Congress of Neuroscience, August 4–9, 1991, Montreal, Canada (Abstract P7.19, p. 66).

We thank Joe Frey for preparing the brain slices; David Tank for important suggestions; and Alan Gelperin, David Kleinfeld, Charles Nicholson, and Rafael Yuste for a critical reading of the manuscript. Support was provided by National Institutes of Health Grants NS13742 and AG09480.

1. Llinás, R. & Hess, R. (1976) *Proc. Natl. Acad. Sci. USA* **73,** 2520–2523.
2. Llinás, R. & Sugimori, M. (1980) *J. Physiol. (London)* **305,** 171–195.
3. Ross, W. N. & Werman, R. (1987) *J. Physiol. (London)* **389,** 319–336.
4. Tank, D. W., Sugimori, M., Connor, J. A. & Llinás, R. (1988) *Science* **242,** 773–777.
5. Sugimori, M. & Llinás, R. (1990) *Proc. Natl. Acad. Sci. USA* **87,** 5084–5088.
6. Stuart, G. (1994) *Neuron* **13,** 703–712.
7. Eilers, J., Augustine, G. J. & Konnerth, A. (1995) *Nature (London)* **373,** 155–158.
8. Yuste, R. & Denk, W. (1995) *Nature (London)* **375,** 682–684.
9. Llinás, R. (1995) *Nature (London)* **373,** 107–108.
10. Kashiwabuchi, N., Ikeda, K., Araki, K., Hirano, T., Shibuki, K., Takayama, C., Inoue, Y., Kutsuwada, T., Yagi, T., Kang, Y., Aizawa, S. & Mishina, M. (1995) *Cell* **81,** 245–252.
11. Denk, W., Strickler, J. H. & Webb, W. W. (1990) *Science* **248,** 73–76.
12. Denk, W., Delaney, K. R., Gelperin, A., Kleinfeld, D., Strowbridge, B. W., Tank, D. W. & Yuste, R. (1994) *J. Neurosci. Methods* **54,** 151–162.
13. Denk, W., Piston, D. W. & Webb, W. W. (1995) in *The Handbook of Confocal Microscopy*, ed. Pawley, J. (Plenum, New York), Chap. 28.
14. Llano, I., DiPolo, R. & Marty, A. (1994) *Neuron* **12,** 663–673.
15. Kuno, M., Maeda, N. & Mikoshiba, K. (1994) *Biochem. Biophys. Res. Commun.* **199,** 1128–1135.
16. Palay, S. L. & Chan-Palay, V. (1974) *Cerebellar Cortex* (Springer, New York).